Facies (2005) 51: 522–540
DOI 10.1007/s10347-005-0065-6

ORIGINAL ARTICLE

Diethard Sanders · Karl Krainer

Taphonomy of Early Permian benthic assemblages (Carnic Alps, Austria): carbonate dissolution *versus* biogenic carbonate precipitation

Received: 21 December 2004 / Accepted: 1 April 2005 / Published online: 7 June 2005

Abstract During the Early Permian, in the area of the Carnic Alps, a quartz-gravelly beach fringed a mixed siliciclastic-carbonate lagoon with fleshy algal meadows and oncoids; seaward, an ooid shoal belt graded down dip to a low-energy carbonate inner shelf with phylloid algal meadows. In limestones, foraminiferal biomurae and bioclast preservation record tapholoss by rotting of non-calcified organisms (interpreted as fleshy algae) and by dissolution of aragonitic fossils. Carbonate loss by dissolution was counteracted and, locally, perhaps exceeded by carbonate precipitation of encrusting foraminifera and as oncoids. Sites of abrasion and carbonate dissolution (beach), sites with tapholoss by rotting and dissolution, but with microbialite/foraminiferal carbonate precipitation (lagoon, inner shelf), and sites only of carbonate precipitation (ooid shoals) co-existed on discrete shelf compartments. Compartmentalized, contemporaneous carbonate dissolution and precipitation, to total amounts yet difficult to quantify, impede straightforward estimates of ancient carbonate sediment budget.

Keywords Permian · Southern Alps · Taphonomy · Carbonate budget · Calcium carbonate dissolution

Introduction

In some recent shallow-water carbonate environments, a significant proportion of magnesian calcite and/or aragonite is dissolved within the unlithified sediment (Moulin et al. 1985; Walter and Burton 1990; Ku et al. 1999; Powell et al. 2002). Marked taphonomic loss of aragonitic and, locally, also of calcitic hardparts is documented for Palaeozoic and Mesozoic neritic successions (Sanders 1999, 2001; Cherns and Wright 2000; Wright et al. 2003). Early dissolution can be recognized by taphonomic, textural and compositional criteria (Sanders 2003) but, in shallow-water environments, tends to be masked by bioturbation, fragmentation, abrasion, micritization and boring. This may explain why, for neritic carbonates and relative to deep-water limestones, syndepositional dissolution was geologically recognized quite late (Sanders 2004). Encrustation of soft or hard substrates by organisms secreting calcium carbonate is long known as an indicator of taphonomic loss (e.g., Voigt 1966; Palmer et al. 1988). In the Lower Permian succession of the Carnic Alps (Fig. 1), shallow neritic limestones with abundant crusts and biomurae composed mainly of the interpreted sessile milioline foraminifer *Ellesmerella* are present (Vachard and Krainer 2001; cf. Flügel and Flügel-Kahler 1980). Miliolines secrete microcrystalline magnesian calcite more resistant to dissolution than aragonite (cf. Murray and Alve 1999). As shown herein, most of the encrustation substrates were represented by fleshy algae, bivalves, phylloid algae, gastropods, and vanished organisms of unknown affiliation. Combined sedimentologic and taphonomic criteria indicate that limestone beds composed of abundant sessile foraminiferal crusts represent lags of syndepositional dissolution that nearly totally eradicated molluscs and phylloid algae, whereas bioclasts of primary calcite (e.g., brachiopods) were preserved. Both the foraminiferal biomurae and partly dissolved bioclasts allow for quantitative estimates of localized minimum amounts of dissolution. Substantial taphonomic loss occurred during deposition of certain intervals, whereas for other intervals, no taphonomic loss was identified. The crusts of interpreted foraminiferal origin represented a significant source of calcium carbonate. Our case study underscores that taphonomic loss and detraction from carbonate budget by syndepositional dissolution is confined to specific depositional settings, precluding straightforward estimates of ancient carbonate budgets.

D. Sanders (✉) · K. Krainer
Faculty of Geo- and Atmospheric Sciences, University of Innsbruck,
Innrain 52,
A-6020 Innsbruck, Austria
e-mail: Diethard.G.Sanders@uibk.ac.at
Tel.: +43-0512-507-5584
Fax: +43-0512-507-2914

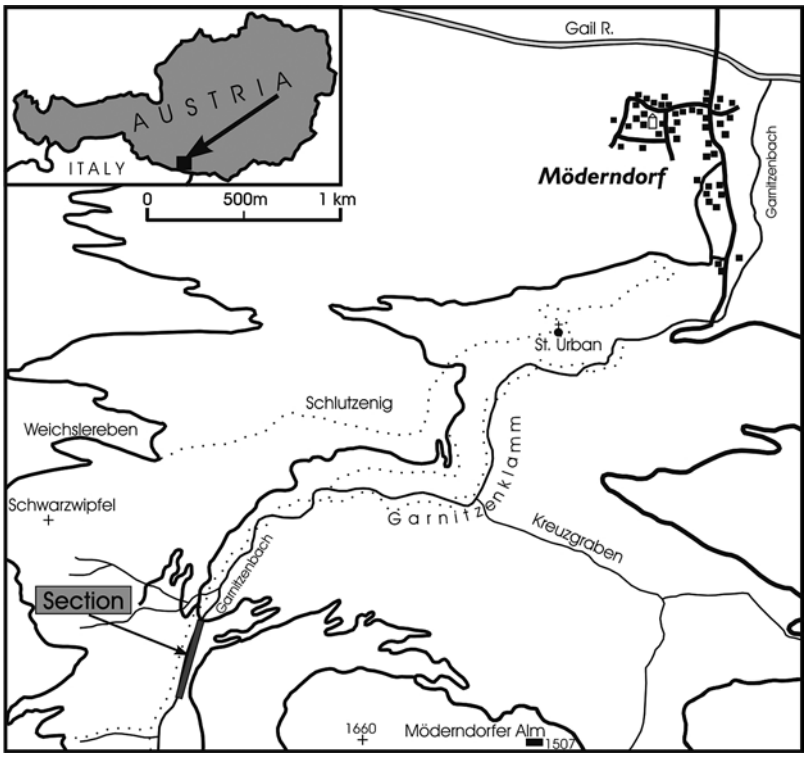

Fig. 1 Geographic location of the investigated succession in Austria

Methods

The percentage of phylloid algal plates in two thin section photographs of typical algal floatstones was measured. Quantification was done by tracing the outline of the algal plates by lines, then quantifying matrix and percentage algae with the pixel count function of the program Adobe Photoshop (Fig. 2). For partly dissolved phylloid algal plates, dissolution was quantified in four thin sections. First, the outline of the preserved portion of the algal plate was traced by lines. The resulting area again was quantified by the pixel count function. Next, the former outline of the algal plate was approximated by lines. Because the algal plates are of fairly simple shape in thin section, the error introduced by this approximation is minimal. The area of the reconstructed algal plate was measured, too. The difference between the preserved and the reconstructed area yields the dissolved portion (Fig. 2).

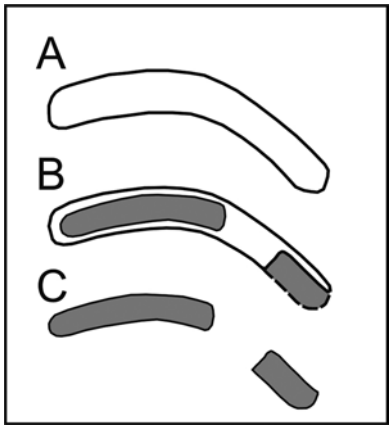

Fig. 2 Method for quantitative estimate of dissolution loss from bioclasts. First, the outline of the bioclast (A) and of potential dissolution cavities (B) is line-drawed on a photograph. **A** Entire bioclast (e.g., a phylloid algal plate): the area can be determined electronically by pixel count. **B** Bioclast with cavities (grey) removed by early dissolution. **C** Area lost by dissolution from the bioclast shown in A: the area lost by dissolution is again determined by pixel count (compare also Figs. 10E–H)

Geological Setting

In the Carnic Alps, a folded Variscan basement of Upper Ordovician to Lower Carboniferous marine sedimentary rocks is unconformably overlain by a marine, mixed siliciclastic-carbonate succession of Late Carboniferous to Early Permian age (Fig. 3). This succession accumulated in basins formed by extension and strike-slip, subsequent to Variscan orogenesis (Venturini 1982, 1991; Krainer 1992). The section described in this paper represents a portion of the upper part of the Rattendorf Group (Fig. 3), i.e., the upper part of the Grenzland Formation and the lower part of the Zweikofel Formation (Fig. 4). The Rattendorf Group is up to about 450 m thick, and includes sandstones and conglomerates of shore zone environments, siliciclastic tempestites, lime-muddy mounds and thickets rich in calcareous algae, and other types of shallow-water limestones (see below; Flügel 1971, 1977; Flügel et al. 1971, 1997; Homann 1972; Forke 1995, Krainer and Davydov 1998; Vachard and Krainer 2001). The Rattendorf Group

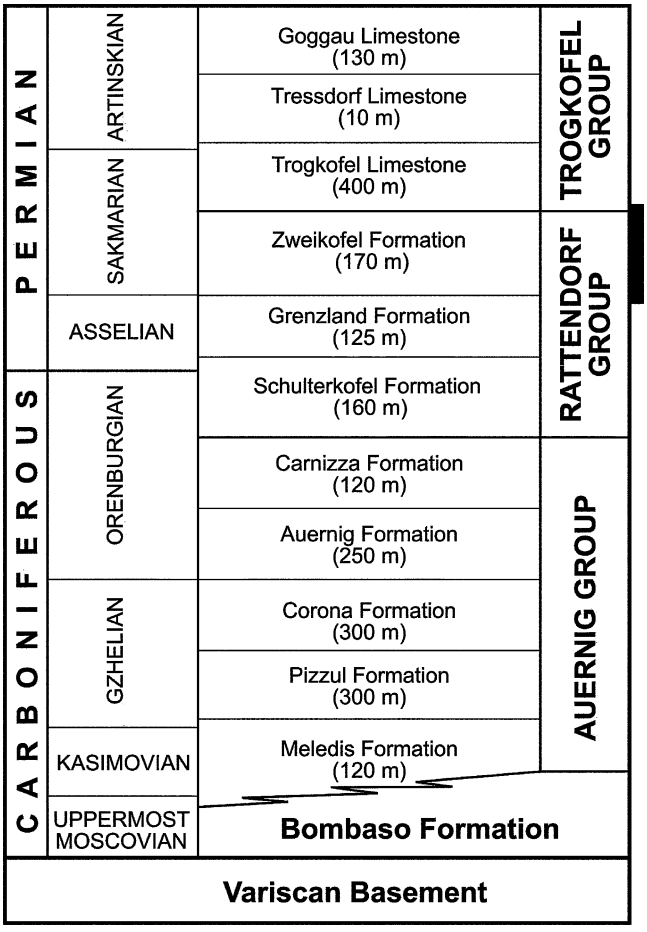

Fig. 3 Upper Palaeozoic of the Carnic Alps. Black bar shows range of section in Fig. 4A

throughout consists of transgressive-regressive, mixed siliciclastic-carbonate packages (cf. Fig. 4). During accumulation of the Grenzland Formation, depositional water depths were similar to the under- and overlying formations in the Rattendorf Group, but terrigenous input was higher (Flügel 1974). The upper part of the Grenzland Formation pertinent for the present paper probably accumulated in more proximal position closer to shore than the Zweikofel Formation (see more detailed description of Garnitzenbach section below). The Rattendorf Group accumulated in an aragonite sea (cf. Stanley and Hardie 1998) near the palaeo-equator (Manzoni et al. 1989), in a climate that allowed for substantial terrigenous input by runoff from land (Buggisch et al. 1976; Krainer 1992). As discussed by Samankassou (2002), in the Upper Carboniferous of the Carnic Alps, a marked paucity of corals and a "foramol" skeletal assemblage combined with an abundance of large microbialitic oncoids and presence of oolites and calcareous green algae indicates that elevated nutrient input by terrestrial runoff precluded, both, formation of larger coral-dominated buildups and pure carbonate deposition. As outlined below, a similar reasoning applies to the Lower Permian succession described herein.

Ellesmerella: characterization

By far the most abundant type of calcified encrustation found in the considered stratigraphic interval (see Figs. 3 and 4) is assigned to the calcitornellid (suborder Miliolina) foraminifer *Ellesmerella* (Fig. 5; cf. Vachard and Krainer 2001). In the investigated succession, *Ellesmerella* has previously been interpreted as the cyanobacterial precipitate *Girvanella* (Flügel and Flügel-Kahler 1980). Relative to *Girvanella*, however, *Ellesmerella* differs in that it is composed of very dense, dark grey, micritic calcium carbonate with a systematic, parallel array of sharply defined tube-shaped constructional voids, whereas in *Girvanella*, the calcified sheaths are very thin and "tangled" (cf., e.g., Riding 1991; Pratt 2001; Rodriguez 2004). In addition to *Ellesmerella*, other types of interpreted milioline foraminifera are present, albeit in lower abundance, that show a similar wall of dense, dark-grey microcrystalline calcium carbonate (Kochansky-Devidé 1973). *Ellesmerella* forms crusts of dark grey, micritic calcium carbonate riddled by regularly-spaced, thin tubes that are parallel both to each other and relative to the encrusted substrate. Thin crusts of *Ellesmerella* may host a single layer of tubes only, but most crusts are thicker and consist of stacked tube layers (Fig. 5). Crusts of *Ellesmerella permica* (Pia 1937) emend. Mamet et al. 1987 (= *Girvanella subparallela* Flügel and Flügel-Kahler 1980: Pl. 11, Figs. 1, 2 and 4) consist of up to about twenty layers of tubes that are 500–700 μm in length and about 80–100 μm in diameter. As described below, *Ellesmerella* formed encrustations on diverse substrates ranging from hard and brittle (such as mollusc shells) to, presumably, firm and tenuous, such as phylloid algal plates, to soft fleshy algae. In many cases the crusts biomurated their substrate. Both large fragments of *Ellesmerella* crusts and the biomurae record the former presence of fossils or fossil fragments that had been largely or completely removed by biostratinomic processes, and represent a significant source of calcium carbonate.

Sedimentary facies

Limestones

In the section described herein, five groups of carbonate facies are distinguished (Table 1). (1) Limestones rich in or composed of crusts and/or biomurae of *Ellesmerella* ("ellesmerellites") show a texture of bioturbated wacke-packstone to, more rarely, partly "washed" bioturbated packstone (see below for further description). Some ellesmerellites are composed of both abundant fragments of *Ellesmerella* crusts/biomurae, and of other sessile foraminifera (mainly *Calcitornella, Calcivertella, Ramovsia*). In the ellesmerellites, the sessile foraminifera occur as isolated bioclasts devoid of their former substrate. (2) Bioclastic limestones include pure to sandy wacke-pack-grainstones (Fig. 6A) or, more rarely, mollusc floatstones (Fig. 6B). In the bioclastic limestones, variable

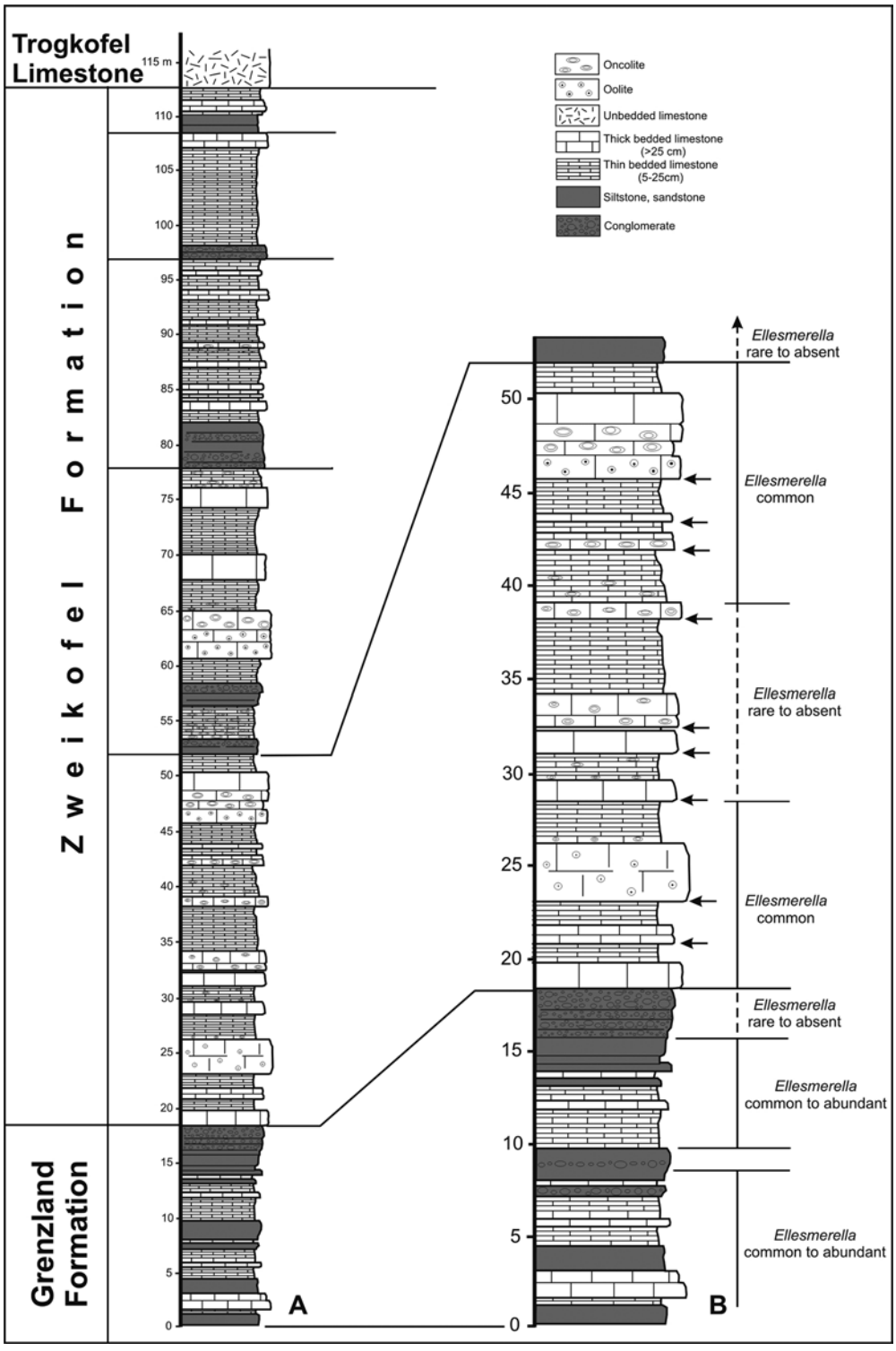

Fig. 4 Succession indicated by black bar in Fig. 3. **A** Upper part of Grenzland Formation to base of Trogkofel Limestone in Garnitzen gorge. The succession consists of shallow neritic siliciclastics and limestones (Table 1). **B** The Grenzland Formation is topped by an interval of shoreface sandstones to quartz-gravelly beachface conglomerates. In the lower part of the Zweikofel Formation, the arrowtips indicate packages of limestones of different facies that are arranged in a vertically repetitive fashion. Intervals wherein crusts and biomurae of *Ellesmerella* are common to abundant are indicated

Table 1 Sedimentary facies in the lower and middle part of Garnitzenbach section

CARBONATE ROCKS	Textures	Typical constituents	Interpretation
Ellesmerella limestones ("ellesmerellites")	Wackestone, packstone, partly "washed" packstone (more rarely)	A: fragments of *Ellesmerella* crusts, smaller benthic foraminifera, fragments of sessile foraminifera, *Ramovsia*; F-R: shells of bivalves and gastropods, microgastropods, productids	Fleshy algal meadows with epibiontic foraminifera
			Lime-muddy substrate with fleshy algae overgrown by sessile foraminifera; substrate colonized by benthic foraminifera, molluscs and brachiopods. Shallow, low-energy subtidal environment of elevated nutrient level
Bioclastic limestones	Wackestone, packstone, grainstone, floatstone	Variable mix of: A-C: phylloid algal fragments, schwagerinids, bivalves, (micro-)gastropods, smaller benthic foraminifera; C-F: brachiopods, crinoid fragments, bryozoans; fragments of Ellesmerella crusts; F-R: *Tubiphytes*, micro-oncoids	Lime-muddy bioclastic sand
			Lime-muddy to bioclast-sandy, bioturbated substrata, low to moderate energy, episodic high-energy events. Perhaps local phylloid algal stands
Phylloid algal limestones	Floatstone, rudstone, bafflestone (more rarely)	A: phylloid algal plates; C-F: sessile foraminifera (incl. *Ellesmerella*), encrusting bryozoans, brachiopods, few small bivalves, (micro)gastropods	Phylloid algal meadows
			Phylloid algal meadows on substrate of lime mud to bioclast-bearing lime mud with. Well-lit, low-energy shallow subtidal of low nutrient level Algal species/genera: *Archaeolithophyllum missouriense, Anchicodium, Neoanchicodium, Anthracoporella, Epimastopora, Pseudoepimastopora, Macroporella, Atractyliopsis, Mizzia, Gyroporella, Connexia*
Oncolites	Floatstone, rudstone	A-C: Variable mix of piso- to macro-oncoids, schwagerinids, smaller benthic foraminifera, phylloid algal fragments, bivalves, (micro-) gastropods,	Oncoid "grounds"
			Substrata of bioturbated, bioclast-sandy lime mud with cyanobacterial pisoids to macroids. Moderate energy, shallow subtidal punctuated by high-energy events

Table 1 Continued

CARBONATE ROCKS	Textures	Typical constituents	Interpretation
Oolites (oolithic to oobioclastic limestones)	Grainstone, packstone	A: ooids; C-R: bioclasts	Ooid sand bars Ooid bars in shallow subtidal environment. Moderate to persistently higher water energy closely below to within fair-weather wave base
SILICICLASTIC ROCKS	Texture, sedimentary structures	Typical constituents	Interpretation
Silstone to sandstone	Unbedded to indistinctly parallel-bedded, indistinctly horizontally laminated	A: Mono- and polycrystalline quartz; R-C: Bioclasts; R: fragments of sedimentary, metamorphic and volcanic rocks	Lower shoreface deposits
Conglomerate	Unbedded to indistinctly subhorizontally bedded, clasts well-rounded, moderately to poorly sorted (matrix support) or moderately to well-sorted (clast support)	A: Quartz gravels; R: Bioclasts	Upper shoreface to beachface deposits

A: abundant; C: common; F: few; R: rare

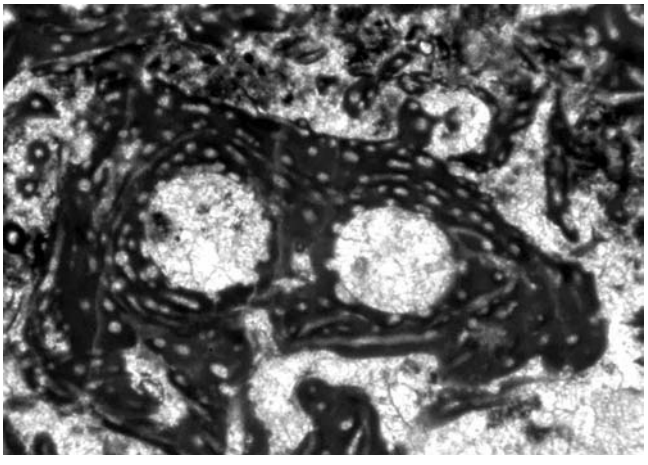

Fig. 5 Crust of *Ellesmerella* (dark grey) interpreted as a sessile milioline foraminifer. The foraminifer grew on vanished encrustation substrates of circular cross-section. Zweikofel Formation, Garnitzenbach section. Width of view 3.5 mm

proportions of phylloid algal fragments, fusulinaceans, and of microgastropods and other mollusc bioclasts are most common. A few bioclasts may bear *Ellesmerella* crusts; in addition, isolated fragments of *Ellesmerella* crusts and murae are fairly common. In many cases, fragments of phylloid algae (see discussion in Baars and Torres (1991) for use of the term) are most abundant, but commonly are nearly completely recrystallized. Algal fragments with preserved microstructure are assigned to the codiaceans *Anchicodium* and *Neoanchicodium*. In addition, fragments of dasycladaceans (mainly *Epimastopora alpina*) are locally abundant. Although a few larger crinoid fragments are present in many beds, bioclastic limestones dominated by crinoid ossicles comprise a few beds only. (3) Phylloid algal limestones include floatstones to lime-muddy rudstones rich in phylloid algal plates (Figs. 6C and D). A total of 11 algal genera includes both phylloid algae and dasycladaleans (Table 1; Homann 1972; Vachard and Krainer 2001). The matrix typically is a lime mudstone to bioclastic wackestone with a low-diversity assemblage of smaller benthic foraminifera (Vachard and Krainer 2001), small brachiopods, and a few fenestrate bryozoans. Most of the algal plates are devoid of encrustations, but local patches of sessile foraminifera, encrusting bryozoans, serpulids and thin crusts of *Ellesmerella* are fairly common (Figs. 6E and F). (4) Onco-float/rudstones are dominated by piso- and macro-oncoids of *Osagia* type (Fig. 6G). The matrix commonly is a pack/grainstone with abundant micro-oncoids, bioclasts and reworked *Ellesmerella* crusts. Oncoid nuclei typically are phylloid algal fragments; other nuclei, such as dasycladalean fragments or gastropods, are rare. Micro-oncoids typically contain small gastropods, phylloid algal fragments, or mollusc fragments. All oncoid cortices consist largely of grey lime mudstone with well-preserved, wrinkly, sub-millimetre lamination; the cortices most probably were produced by calcification of cyanobacterial biofilms (cf. Riding 1991). By sediment composition, there exists a gradual transition from phylloid algal limestones to oncolites. (5) Oolites include oolithic to oobioclastic grainstones and, less commonly, packstones. There also exist gradual transitions from oncolites to oolites. In the investigated section, no evidence for vadose diagenesis or subaerial exposure has been identified, such as micritic meniscus cements, microkarst, emersion surfaces or abrupt vertical shifts of facies indicative of sea-level fall.

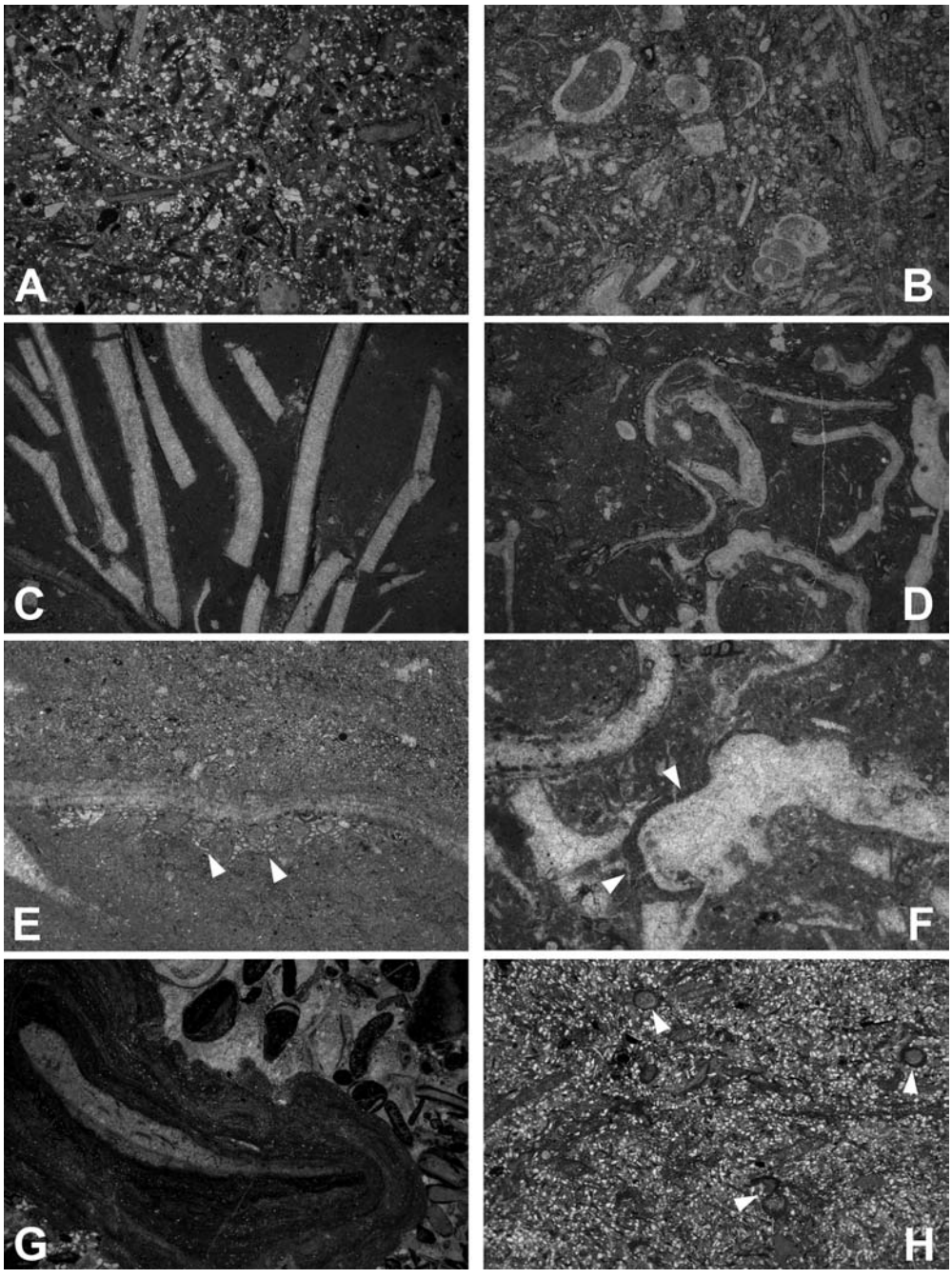

Fig. 6 Limestones of upper part of Grenzland Formation and lower part of Zweikofel Formation. **A** Bioturbated bioclastic packstone with a few percent of siliciclastic silt to sand. Grenzland Formation. Width 17 mm. **B** Bioturbated floatstone with microgastropods and fragments of mollusc shells and phylloid algal plates. Grenzland Formation. Width 17 mm. **C** Phylloid algal floatstone with matrix of lime mudstone. Note sharp, intact edges of algal plate fragments and the scarcity to absence of encrustation. In this image, phylloid algal plates occupy about 27% of total area. Grenzland Formation. Width 17 mm. **D** Phylloid algal floatstone with intact algal plates. Zweikofel Formation. Width 17 mm. **E** Phylloid algal plate encrusted by bryozoan (marked by arrowtips). Grenzland Formation. Width 6.5 mm. **F** Detail of **D**. Phylloid alga, overgrown by *Ellesmerella* crust (marked by arrowtips). Zweikofel Formation. Width 5.3 mm. **G** Onco-rudstone with matrix of rounded bioclastic grainstone. As typical for the succession, the nucleus of the oncoid is a phylloid algal plate. Grenzland Formation. Width 17 mm. **H** Well-sorted, bioturbated, siltstone with tube-shaped biomurae (marked by arrowtips) of *Ellesmerella*, and with fragments of phylloid algae and crinoids. Grenzland Formation. Width 8.5 mm

Siliciclastics

Siliciclastic rocks are represented by lime-muddy siltstones, fine- to coarse-grained sandstones, pebbly sandstones, and fine-grained conglomerates (Table 1). Fine-grained sandstones are moderately to well-sorted; coarse-grained sandstones are poorly sorted. Sand grains are mostly angular to subangular, larger grains are

subrounded to rounded. All siliciclastic lithotypes are cemented by blocky calcite spar that randomly replaces detrital quartz and feldspars. Whereas mono- and polycrystalline quartz grains are most abundant, grains of sedimentary chert, schistose metamorphic rocks, basaltic volcanics, sandstone and recrystallized carbonates are less common. In all samples, small amounts of detrital micas (mainly muscovite) are present. Siltstones to sandstones commonly are bioturbated, and most contain bioclasts such as mollusc shell debris, smaller benthic foraminifera, and fragments each of crinoids, fusulinaceans, calcareous algae, crusts of *Ellesmerella* (common in some beds; Fig. 6H), bryozoans, and brachiopod spines. Rarely, fragments of coalified wood are present. Mixed siliciclastic-carbonate arenites contain abundant fossil fragments and micritic lithoclasts displaying dark micritic rims ("coated grains"), and a few micritic intraclasts. This lithotype locally grades into bioclastic wackestone containing up to 20% siliciclastic grains. The siltstones to sandstones probably accumulated in a lower shoreface to transitional environment. Intervals of beachface conglomerate are up to 1 m thick, and consist of or are rich in well-rounded, fine to medium-grained gravels of quartz; rounded shallow-water bioclasts are very rare. Polymictic conglomerates rich in sedimentary rock fragments are rare. Clast-supported conglomerates consist of moderately to well-sorted, fine to medium gravel; conversely, conglomerates supported by siliciclastic sandstone contain poorly sorted, scattered quartz pebbles up to coarse gravel size. Some intervals of beachface conglomerate show a sharp, erosive base.

Garnitzenbach section

Description

In its lower 18 m, representing the upper part of the Grenzland Formation, the section consists of subequal amounts of limestones and siliciclastics (Fig. 4B). Most of the limestones are slightly argillaceous to sandy, bioturbated bioclastic wacke/pack/floatstones. Bioturbated bioclastic grainstones and onco-rudstones are common in two intervals (Fig. 4B), but may also be intercalated in discrete beds up to about 30 cm thick between other lithologies. Limestone beds of "ellesmerellites" are present mainly in the lower part of the section, in vertical association with shore zone siltstones to sandstones that, too, may be rich in *Ellesmerella* crusts (Fig. 6H). Within a few beds of bioturbated limestone or siltstone, scattered quartz gravels are present. On a vertical scale of a few metres, the limestones and the silt- and sandstones overlie each other without obvious cyclicity. In the topmost four metres of the Grenzland Formation, a package is present that consists, in its lower part, of siltstone, sandstone, and of a bed composed of both quartz gravels and abraded macro-oncoids, whereas the upper part is an interval about 2.5 m thick of quartz-gravelly beachface conglomerate.

With respect to the inventory of facies, the overlying Zweikofel Formation is similar to the Grenzland Formation, but the vertical arrangement and relative thickness of facies are different. In its lower 65 m, the Zweikofel Formation consists of distinct stratal rhythms each a few metres thick (Fig. 4A). Each rhythm consists of (a) an interval of thick-bedded oolites and/or of bioclastic grainstones to oncolites, and (b) an interval of medium- to thin-bedded phylloid algal floatstones and bioclastic wacke/packstones. The stacking of these rhythms is not associated with a clear-cut, higher-order shift of facies. In addition, shallow-marine clastics are present and include siltstones, sandstones and quartz conglomerates. The intervals of clastics, however, are intercalated in larger vertical distances than set by the carbonate rhythms, and their presence is not associated with the vertical rhythmicity of limestone bedding and facies. In the upper 30 m of the Zweikofel Formation, rhythmicity is also present, but subdued, and the succession is dominated by medium- to thin-bedded bioclastic packstones (Fig. 4A). In the entire described section, macroboring of fossils and other substrates (e.g., oncoids) overall is very rare. Although a few fragments of *Ellesmerella* crusts are present in many limestone beds, intervals with abundant *Ellesmerella* are confined to more-or-less discrete levels within the lower 52 m of the section (Fig. 4B).

Interpretation

The described facies and their vertical arrangement are placed in a reconstruction of the shore zone to inner shelf during deposition of the upper Grenzland and the lower to middle part of the Zweikofel Formation, respectively (Fig. 7). As mentioned, the beachface conglomerates in the Garnitzenbach section are sharp-based, and some intervals show erosion at their base. In addition, a few kilometres to the west of the investigated section, at the type location of the Zweikofel Formation, distinctly erosive-based intervals of quartz-gravelly beachface conglomerates incised into shallow subtidal limestones are present. Both in the Garnitzenbach section and at Zweikofel, thus, the shore zone clastics are interpreted as records of sea-level drawdown, perhaps related to the active tectonic deposetting (see above), and/or to waxing and shrinking of Late Carboniferous to Early Permian Gondwanian ice sheets (cf. Frakes et al. 1992; Scotese et al. 1999). According to Ross and Ross (1985), Upper Carboniferous to Lower Permian cyclothems can be correlated globally. The glacio-eustatic nature of these cyclothems is also supported by statistical tests (Algeo and Wilkinson 1988). Because sharp-based shore zone deposits are one diagnostic feature of forced regression by active sea-level fall (e.g., Plint 1988; Pattison 1995), we interpret the cycles as influenced by glacio-eustasy.

The described upper part of the Grenzland Formation accumulated mainly in a shallow subtidal, "lagoonal" environment of low water energy, as indicated by the prevalent wacke/pack/floatstone texture of limestones. Episodic high-energy events are recorded by the scattered quartz gravels within other lithologies, and by intercalated beds of bioclastic grainstones and onco-rudstones. The ellesmerellites, however, represent a (par)autochthonous

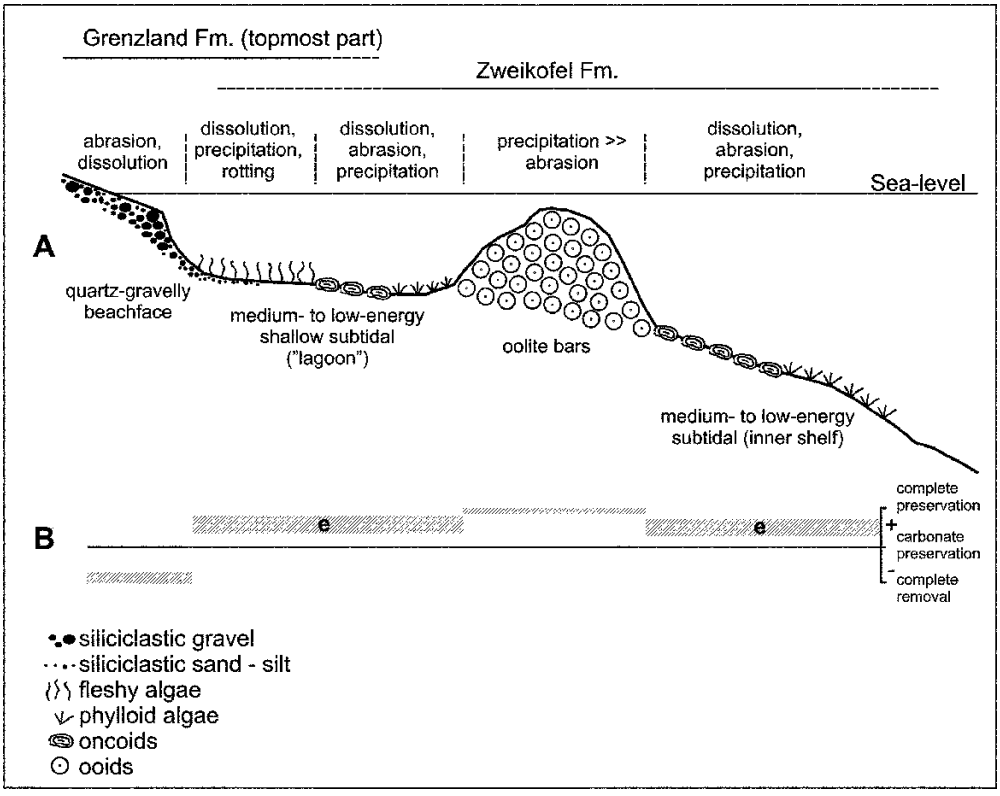

Fig. 7 Schematic reconstruction (vertically exaggerated, not to scale) of depositional environments pertinent for the succession shown in Fig. 4. **A** Benthic assemblages and taphonomic regimes. See text for further description and discussion. **B** Preservation (schematic) of calcium carbonate in relation to depositional setting. Shaded bars indicate approximate range of carbonate preservation. Bars labelled **e** indicate settings with a significant contribution of calcium carbonate by epibionts

facies (see chapter Taphonomy below). In the Grenzland Formation the thin, lower interval of quartz conglomerate, and the two intervals rich in bioclastic grainstone and oncorudstones record phases of higher water energy. The cause, or causes, of such minor changes in water energy and/or clastic input is difficult to assess. Small changes in water energy may result from minor sea-level fall, perhaps dampened by tectonic subsidence, or from changes in local wave climate related to wind regime or to beach dynamics and related patterns of wave refraction (Hampson 2000). As mentioned, the limestones and the silt-sandstones overlie each other without obvious cyclicity. The vertical changes of facies, including changes from siliciclastics to carbonate deposition, probably result from minor shifts of facies in a shallow subtidal, low-energy nearshore environment. The topmost, upward-coarsening package from siltstone to beachface conglomerate, however, records the progradation of a low-energy quartz-gravelly beach.

Above, in the Zweikofel Formation, the prevalence of limestones of similar facies, and the similar nature but scarcer presence of intervals of siliciclastics record diminished terrigenous input. In the lower and middle part of the Zweikofel Formation, the significance of the described stratal rhythms of ooid/bioclastic grainstones or oncolites, and of phylloid algal floatstones and bioclastic wacke/packstones record changes in mean water energy and depth. Because phylloid algae easily disintegrated into small fragments, and because oolites, grainstones and macro-oncolites need agitated, shallow water of moderate to high energy to form, the ooid/bioclastic grainstones or oncolites represent the higher-energy portion of the packages. In the Zweikofel Formation, the absence of a clear-cut, higher-order shoaling or deepening indicates that the deposition of the rhythms was not associated with major shifts of facies and water depth. This is underscored by the intercalated intervals of shore zone clastics. The observation that the siliciclastic intervals are present in larger vertical distances than set by the carbonate rhythms, their "decoupling" from the vertical rhythmicity of limestone rhythmicity, and the sharp-based intervals of shore zone clastics in the type section all suggest that clastic input was controlled by both patterns of sediment dispersal and sea-level drawdown. In the upper part of the Zweikofel Formation, the subdued rhythmicity and the prevalence of bioclastic pack/wackestones may indicate an inner shelf environment ahead of or laterally aside of ooid shoals.

Ellesmerella crusts

Description

According to their appearance in thin section, five types of *Ellesmerella* crusts are distinguished. (1) Platy fragments of gentle to distinct curvature (Figs. 8A–D). (2) "Simple tubes" that are filled, either, by matrix (Figs. 8E and G), or blocky calcite spar (Fig. 8F), or by small geopetals of sediment overlain by calcite spar. Sediment-filled, simple tubes of *Ellesmerella* may be quite delicate (Fig. 6H). A few of the simple tubes are bifurcated (Fig. 8G) or, in longitudinal section, show a closed termination on one side. In thin section, most of the simple tubes appear straight, whereas

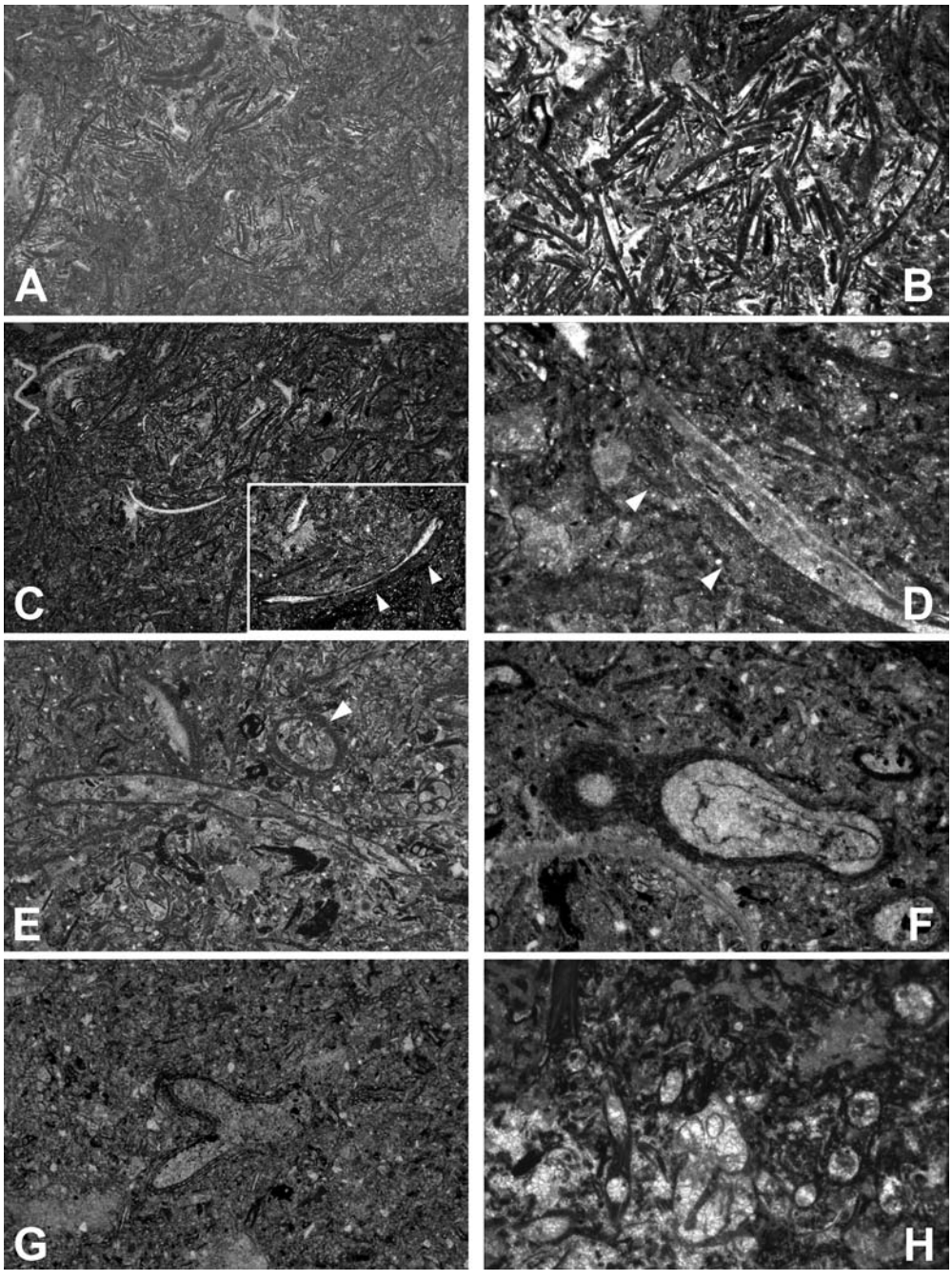

Fig. 8 Types of *Ellesmerella* biomurations. **A** Bioturbated packstone composed exclusively of platy fragments of biomurae built by *Ellesmerella* ("ellesmerellite"). Grenzland Formation. Width 17 mm. **B** Detail of bioturbated packstone to grainstone that consists exclusively of platy fragments of biomurae built by *Ellesmerella* ("ellesmerellite") Grenzland Formation. Width 6.5 mm. **C** Bioturbated packstone ("ellesmerellite") composed of platy fragments of *Ellesmerella* biomurae, and a few shells of brachiopods (light grey). Width 17 mm. Inset delimited by white lines shows one of the very few bivalve shells in this limestone. The shell is biomurated by *Ellesmerella* (indicated by arrowtips). Width of inset 6.5 mm. Grenzland Formation. **D** Portion of bivalve shell with *Ellesmerella* biomura (indicated by arrowtips). The shell has been partly replaced by matrix. Grenzland Formation. Width 3.5 mm. **E** Cross-section of tube-shaped *Ellesmerella* mura (indicated by arrowtip) The large, elongated biomura below may represent a longitudinal section through a tube, or of an oblique section trough a biomurated shell. Note that the biomurae are filled by sediment identical to the matrix they are embedded within. Grenzland Formation. Width 6.5 mm. **F** Section through an *Ellesmerella* biomura that probably encrusted a substrate of curved, or "wound", shape. Grenzland Formation. Width 3.5 mm. **G** Part of *Ellesmerella* biomura that shows an apparently branched pattern. Grenzland Formation. Width 3.5 mm. **H** Microbial boundstone to bafflestone composed of tube-shaped *Ellesmerella* biomurae that, in many cases, are laterally fused. Note that the form of some of the biomurae suggest that the encrusted substrate was (always or facultatively) of curved or irregularly-wound shape. Grenzland Formation. Width 5.3 mm

others probably are curved, as suggested by pinching and swelling in two-dimensional section (Fig. 8F). Quantitative counting of the inner width (lumen) of simple tubes in some thin sections showed no sharp peak, but a range of lumen widths. Lumina ranging from 1 to 1.5 mm or larger, however, are scarce. (3) Simple tubes merged laterally by a single crust in common ("merged tubes"; Fig. 8H). In merged tubes, the long axis of the inner cavity was curved or straight, and the inner cavity is of nearly perfectly circular cross-section (Fig. 8H). Fragments and clusters of merged tubes are abundant only in some samples. (4) "Double tubes" composed of an inner crust and an outer crust that are separated from each other by blocky calcite spar or, more commonly, by matrix (Figs. 9A and B). For the relatively uncommon "double tubes", the same observations as for the simple tubes apply, but a potential curvature of double tubes could not be discerned. No lateral transition from a simple tube into a double tube was found; each type of tube thus seems to represent a discrete type. In some double tubes, an "inward-outward" polarity of *Ellesmerella* growth can be discerned (Fig. 9A). (5) Other, uncommon forms of crusts: The shape of some crusts indicates that they stem from biotic substrates of elongate, pinching and swelling shape. Although overall rare, in some samples these forms of crusts are common (Figs. 9C and D). Rarely, more-or-less plane crusts were found that overgrew a substrate with "chambers" arranged in a pearl-necklace like fashion (Figs. 9E and F). Some of the chambers are delimited by *Ellesmerella* crusts (Fig. 9E).

Interpretation

(1) For the curved platy fragments, their size and radius of curvature and, in some cases, a gradual decrease of curvature along the fragment are reminiscent to both the size and ontogenetic growth curvature of bivalve or brachiopod shells. Thus, the crusts that constitute these fragments probably grew on shells, but now are devoid of their substrate. This interpretation is also supported by the presence of a few shells biomurated by *Ellesmerella* (Fig. 8C). (2, 3) The simple tubes originated from unknown encrustation substrates. If the simple tubes resulted from encrustation of a single taxon, this implies that the differences in the width of the central cavity of the tubes result from differences in ontogenetic maturity and/or in mature body size of the substrate. In this case, the vanished organism should have the shape of a tube, or a string, gaining in width with increasing distance from bottom, and/or with increasing age. As described, however, tubes cut subparallel to their long axis do not show a change of diameter. The longest tube fragment observed that is cut subparallel to its long axis is about 5 mm in length. Rather, the tube shapes and the closed terminations observed in some longitudinal sections suggest that organisms that were of more-or-less constant thickness over most of or their entire length where encrusted. The terminations and bifurcation of at least some of the simple tubes suggest that (some) of the encrusted organisms were branched, perhaps in a dichotomous fashion. Similarly, for the merged tubes, no evidence for a marked change of tube diameter parallel to the long axis was seen. The organisms that provided the substrate for the tube-shaped crusts potentially had aragonitic hardparts that were dissolved away. Animals with aragonitic hardparts that may occur in tube-shaped tests or shells include sessile foraminifera, bryozoans and vermiform gastropods. Vermiform gastropods were present at least since the Devonian, and perhaps since the Ordovician (order Microconchida, Weedon 1991), but the size and shape of the tubes do not fit with this interpretation (cf. Burchette and Riding 1977; Weedon 1990). No Late Palaeozoic sessile foraminifera and bryozoans are known that had an aragonitic test. The bifurcations of the simple tubes may suggest that they originated on (weakly) calcified aragonitic green algae. No relictic structures suggestive of former calcification were observed; in a large sample number, however, this may be expected (cf. Sanders 2003, and below). Alternatively, the encrustation substrates were devoid of hardparts. Similarly, the interpreted milioline foraminifer *Ramovsia* had also encrusted unpreserved, tubular substrates. We thus consider it most probable that the tubes built by the sessile foraminifera crusts originated from encrustation of fleshy algae (see also Kochansky-Devidé 1973; Flügel and Flügel-Kahler 1980). This is consistent with the described size and shape of tubes, with the frequency distributions of tube width and, perhaps, also with tube bifurcations. It is probably also consistent with the abundance of sessile foraminifera that occur isolated in the beds of ellesmerellite. Even in very calm settings, algae nearly constantly move. We infer that foraminiferal encrustation started from the base of the alga, and/or from sessile foraminifera attached to algal stems.

(4) The comparatively rare double tubes (Figs. 9A and B) may result from encrustation of an organism with a central cavity separating an outer and an inner surface. Although dasycladalean algae are characterized by a central channel, in those cases where dasycladaleans are encrusted by *Ellesmerella*, even in case of nearly complete dissolution, clear-cut ghost fabrics of the former algae are present (see also Sanders 2003). For geometrical reasons, it is precluded that the double tubes represent a cutting effect trough strongly curved substrates, such as potentially were provided by gastropod shells. The polarity of *Ellesmerella* growth (Fig. 9A) suggests that, in the double tubes, each of the encrustation surfaces was an outer surface, and an outer surface only. (5) The crusts that show systematic pinching and swelling (Figs. 9C and D) may have grown on another kind of fleshy alga or, perhaps, on small non-skeletal sponges. In the plane crusts that overgrew a substrate with "chambers" arranged in a pearl-necklace like fashion, the observation that some of the empty chambers are delimited by *Ellesmerella* crusts (Fig. 9E) suggests that these crusts may have grown contemporaneously with their substrate. In summary, whereas by far most of the *Ellesmerella* crusts demonstrably grew on shells and on phylloid algae (curved platy fragments), others probably grew on fleshy algae (simple tubes, pinch-swell tubes?, double tubes?) and/or perhaps on small sponges (pinch-swell tubes?, double tubes?, "pearl-necklace" patterns?).

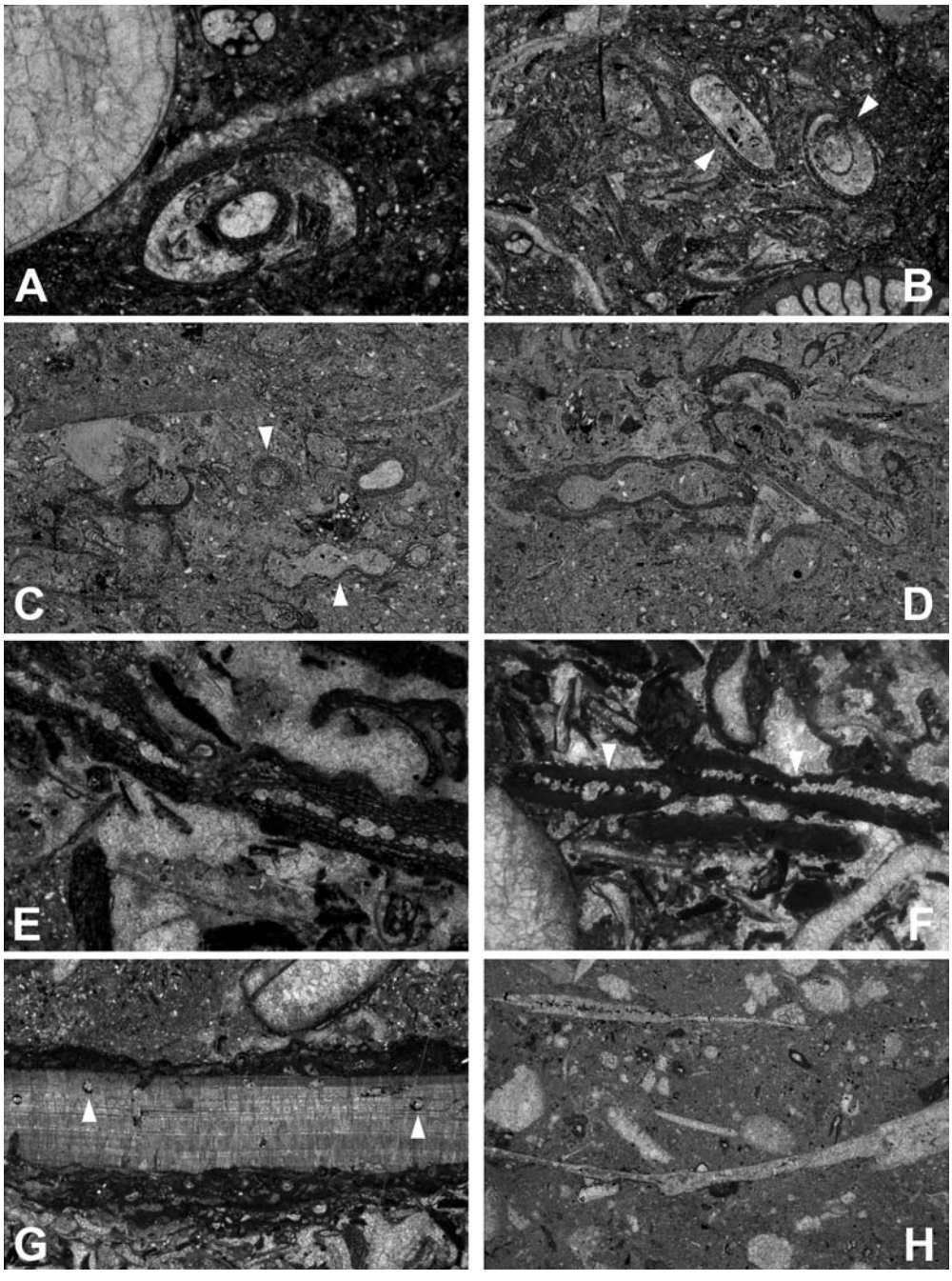

Fig. 9 Types of *Ellesmerella* biomurations (continued). **A** Partly crushed "double-ring" of *Ellesmerella* biomurae. The sharp inner and the irregular outer boundary of the biomurae indicates that each of the crusts grew outward from its substrate. Grenzland Formation. Width 3.5 mm. **B** Arrowtips indicate a "simple" *Ellesmerella* tube (left) and a "double-ringed" *Ellesmerella* biomura (right). In this sample, "double-ringed" biomurae are common. Note also portion of well-preserved fusulinacean foraminifer in lower right. Grenzland Formation. Width 5.3 mm. **C** Different types of *Ellesmerella* biomurae. Arrowtips indicate a "simple tube" (above) and a "pearl-necklace" shaped biomura (below). Grenzland Formation. Width 8.5 mm. **D** "Pearl-necklace" shaped *Ellesmerella* biomura (left) and elongate, "simple" (?tube-shaped) biomura (right). Grenzland Formation. Width 7 mm. **E** *Ellesmerella* biomura on a vanished substrate of chambers arranged in "pearl-necklace" like pattern in section. Arrowtips indicate chambers delimited by *Ellesmerella* crusts. Grenzland Formation. Width 3.5 mm. **F** *Ellesmerella* biomura on a vanished substrate of "pearl-necklace" like appearance in section. Grenzland Formation. Width 4.2 mm. **G** Bivalve shell of prismatic calcite, murated by sessile foraminifera. Note the irregular and pitted lower margin of the shell, and the small borings (two indicated by arrowtips). Grenzland Formation. Width 6 mm. **H** Mollusc-clastic floatstone, with gastropods and disartikulated shells of bivalves. Many of the mollusc shells show lateral thinning and pinching out unrelated to ontogenetic growth, and an irregular outline of their shape. Grenzland Formation. Width 8.5 mm

Taphonomy

Ellesmerella crusts

The ellesmerellites can be subdivided into two categories, (1) limestones of bioturbated wacke/packstone to partly "washed" packstone texture composed mainly of platy curved crust fragments, and (2) bioturbated wacke/packstones rich in both *Ellesmerella* (curved platy fragments, tubes) and other sessile foraminifera. In ellesmerellites composed mainly of curved platy fragments, a few encrusted shells of bivalves and brachiopods and, in some cases, a few encrusted fragments of both phylloid and dasycladalean algae are present. The shells are encrusted, either, on their outer side only, or both on their outer and inner side. The encrusted bivalve shells are preserved as calcite spar (Fig. 8C), or had been replaced by sediment (Fig. 8D), or are filled by both sediment and calcite spar. In many cases, fragments of *Ellesmerella* crust had collapsed into the space now occupied by calcite spar and/or by sediment. In a few cases thicker, curved platy fragments were observed that are bored and/or that have been overgrown on both sides by sessile foraminifera. In wacke/packstones with *Ellesmerella* and foraminifera, both sessile and smaller benthic foraminifera are common to abundant, in addition to a substantial proportion of variable relative amounts of both curved platy fragments and simple tubes. The infilling of the simple tubes (see above) correlates with sediment texture: in grainstones and in partly washed packstones, most of the tubes are filled by blocky calcite spar. In wacke/packstones, and in bioclastic floatstones, most of the tubes are filled, geopetally or completely, by sediment of identical composition and texture as the matrix. Some of the bioclasts, but mainly the *Ellesmerella* crusts, may be partly to nearly completely replaced by finely crystalline pyrite. Where present, pyritization tends to be most complete along the outer fringe of *Ellesmerella* crusts, or crust fragments. In addition, small crystals of idiomorphic pyrite disseminated in the sediment are fairly common. In total, however, pyrite comprises much less than 1% of the rock.

Other constituents

Brachiopod shells are well preserved, and even on thin, delicate shells and productid spines, no features of abrasion or dissolution were identified. Throughout the investigated section, crusts of sessile foraminifera mainly on shells and phylloid algal plates are widespread, but macroboring is very scarce (Fig. 9G). In many beds of bioclastic wacke/pack/floatstone, mollusc shells commonly show (a) abrupt thinning, (b) irregular pinching and swelling, or (c) pits and steps, each unrelated to ontogenetic growth (Figs. 9G and H). In addition, within dasycladalean stems or phylloid algal plates encrusted by *Ellesmerella*, the inner part of the algae is completely replaced by sediment, or nearly so.

In phylloid algal limestones, the inner part of many or most of the algal plates is riddled by more-or-less wide cavities of highly irregular shape. The cavities are filled by matrix identical to and in physical continuity (*via* local "breaches") with the host matrix. In many cases, only the outer fringe of the algal plates is preserved (Fig. 10A). The thin "relict" fringes of algal plates may have been crushed during bioturbation, producing very small, delicate fragments. Where partly destroyed phylloid algal plates provide the nucleus of oncoids and of foraminiferal/microbialite-encrusted grains, features of dissolution are always confined to the algal plate (Fig. 10B). Locally, where destructional cavities breach the surface of phylloid algal plates, the cavities became "clad out" form-concordantly by the oncoidal encrustation. A protective effect of encrustation is obvious where algal plates had been encrusted only on one side: whereas the encrusted side is preserved intact, the non-encrusted side may have been subject to substantial destruction (Fig. 10C).

In the Garnitzenbach section, dasycladalean algae are distinctly less common than phylloid algae. Where dasycladalean fragments are present as oncoid nuclei, commonly only an outer fringe of the alga is preserved. The preservation of fusulinacean foraminifera is highly variable, both between different beds of limestones and within single rock samples. In general, in the investigated section, good preservation (e.g., Fig. 9B) is less common than preservation in diverse stages of biostratinomic detraction, in particular by abrasion and by disintegration of septae and test walls. In fusulineaceans, disintegration of the test may have started from the inner part, at the comparatively thin septae, or additionally proceeded from the external surface of the test (Fig. 10D). As a result, in many fusulinaceans, the test periphery and the septae are incompletely preserved. Most of the described features of preservation were observed in bioturbated, lime-muddy lithologies. In oolitic to oobioclastic grainstones, by contrast, aside of abrasion and rounding of bioclasts, no clear-cut other features of taphonomic overprint have been observed.

Interpretation

As mentioned miliolines precipitate magnesian calcite that is more resistant to dissolution than aragonite. In the ellesmerellites, the good preservation of shells and tests of original low-magnesian calcite (brachiopods) and magnesian calcite (miliolines), and the marked scarcity and poor preservation of bivalve shells suggest that former aragonitic hardparts were subject to taphonomic loss by aragonite dissolution within the soft to firm sediment. The biomurated bivalve moulds filled by sediment, or by both sediment and calcite spar, are explained as a result of *in situ* dissolution of aragonite below the low-magnesian *Ellesmerella* murae. A protective effect against aragonite dissolution is also indicated by the fragments of calcareous algae (dasycladaleans, phylloid algae) that are preserved mainly adjacent to and below crusts of *Ellesmerella* and below oncoidal microbialite, whereas the larger, inner part of the algal fragments

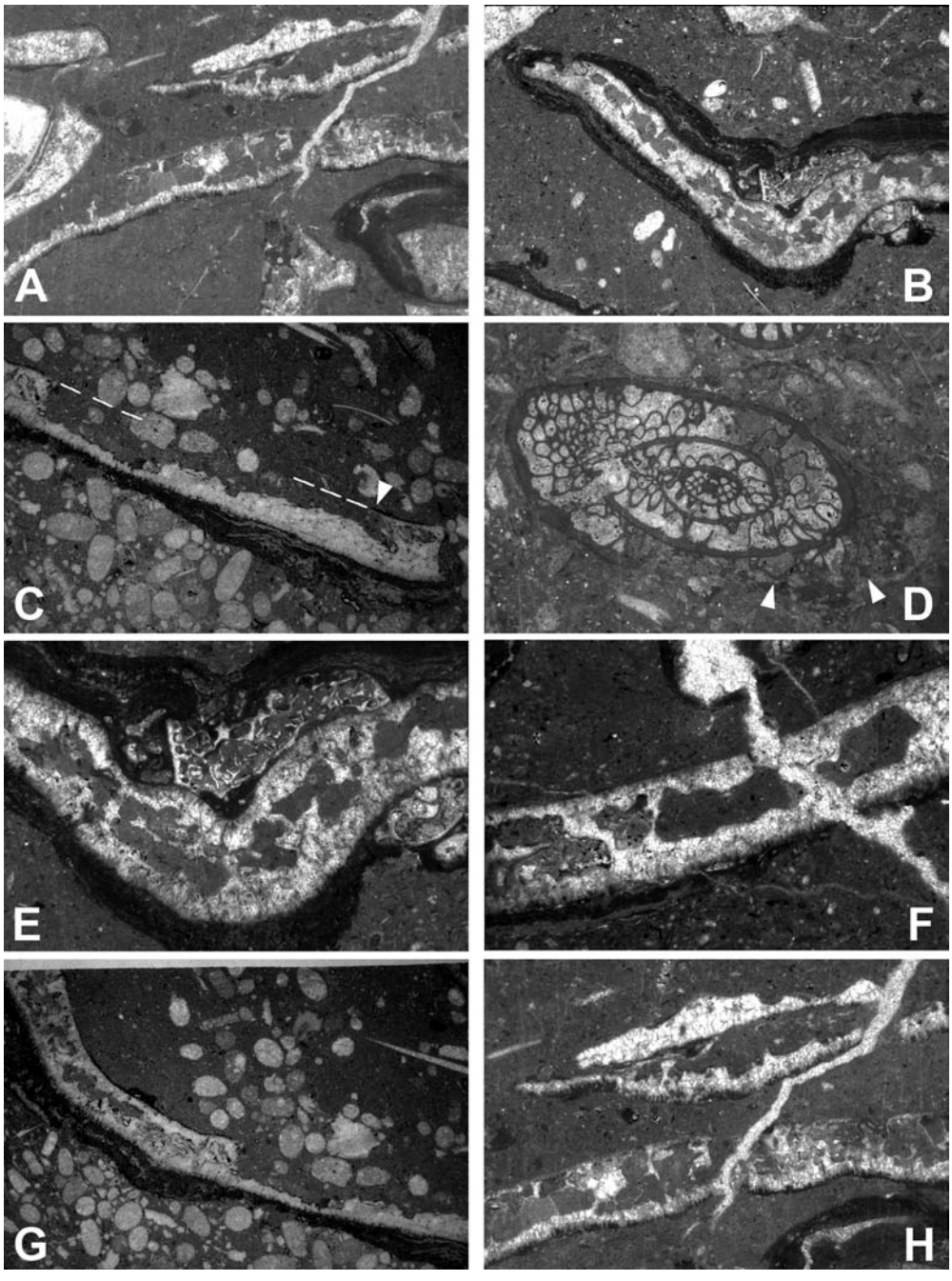

Fig. 10 Records of taphonomic loss by dissolution. **A** Floatstone of phylloid algal plates. Note that the algal plates are thinned and show an irregular outline. Algal plate in centre has been largely dissolved, and the resulting biomould has been filled by a matrix of lime mudstone identical with and, locally, in physical continuity with the matrix in which the algal plates are embedded. Zweikofel Formation. Width 15 mm. **B** Detail of floatstone composed of phylloid algal plate fragments, of algal plates with thin oncoidal coatings (as shown), and of well-developed oncoids with algal plates as nuclei. Note that the phylloid algal plate in photo has been partly dissolved, and the resulting pore space has been filled by matrix of lime mudstone (grey). Zweikofel Formation. Width 17 mm. **C** Phylloid algal plate in center of photo bears an oncoidal (microbialitic) coating on its lower side, whereas the upper part of the algal plate has been largely removed and shows an highly irregular outline. Arrowtip indicates original thickness of algal plate, dashed white line marks approximate outline of formerly intact plate. Zweikofel Formation. Width 15 mm. **D** Fusulinacean foraminifer. The outer whorl has been largely removed, and is indicated only by a few septae (indicated by arrowtips) that remained. Note that also in the inner part of the test, the septae are incompletely preserved. Zweikofel Formation. Width 6.5 mm. **E** Detail of **B**. Shows central portion of phylloid algal plate, with about 32% removed by dissolution. Width 8.5 mm. **F** Phylloid algal plate, with about 37% of the plate dissolved. Zweikofel Formation. Width 6.5 mm. **G** Same sample as in **C**, but showing a different part of the algal plate. In this sector of the plate, about 52% has been removed. Width 17 mm. **H** Detail of **A**, showing the middle part of the algal plate. In this image, about 65% of the plate has been removed. Width 10.5 mm

became replaced by host sediment. For the limestone intervals between the ellesmerellites, the described patterns of preservation of molluscs, phylloid algae and fusulinaceans also record syndepositional dissolution as an important process in taphonomy.

Alternatively, the ellesmerellites rich in or composed of curved platy fragments may have originated by spalling of crusts from shells. If the crusts spalled off bivalve shells either by impact during high-energy events or due to decomposition of the periostracum after death of mussels, hydrodynamic transport of the platy fragments away from bivalve-colonized substrates must be assumed, to explain the marked excess of crusts relative to shells. If hydrodynamic sorting was effective, a more equalized distribution of platy *Ellesmerella* fragments throughout the section may be expected; this is not the case (cf. Fig. 4). Furthermore, relative to bivalve shells, the platy crusts are of highly variable size and, in many cases, of larger thickness, i.e., of variable weight and hydraulic radius. If significant hydrodynamic sorting occurred, thus, one may expect that disarticulated bivalves, bivalve shell fragments and the crust fragments were transported all together. Moreover, if this facies originated mostly by spalling and sorting, we might expect bivalve shell beds with a frequency similar to the ellesmerellites. No bivalve shell bed, however, has been identified in the section. Thus, whereas minor hydrodynamic enrichment of crust fragments is possible, the sum of evidence indicates that it was not the most significant process in the formation of the *Ellesmerella*-rich beds. Moreover, in some samples, overgrowth of curved platy crusts on both sides by sessile foraminifera, and abrasive rounding of crusts indicate that some of the crusts were exposed and transported on the sea floor. In this case, if no dissolution occurred, we might expect a higher proportion of mollusc shells. Some platy fragments most probably also originated from encrustation of dasycladaleans and phylloid algae (cf. Fig. 6F). For the ellesmerellites, we thus infer that bivalves and, to a lesser extent, gastropods were preferentially lost by syndepositional dissolution in the soft sediment. The other types of *Ellesmerella* crusts (see above) record taphonomic loss probably of fleshy algae, calcisponges, and dasycladalean algae.

As obvious from the reconstructed facies belts (Fig. 7), lithologies with abundant *Ellesmerella* and/or with oncoidal microbial crusts were deposited in a "lagoonal" and inner shelf environment. Along the shore, because of the extremely abrasive regime of gravelly beachfaces to upper shorefaces, bioclasts of calcium carbonate were destroyed. Observations on recent beaches indicate that, on low-energy gravelly shores, by far most of the abrasive action occurs during high-energy events, but is effective in grinding down practically all bioclasts (cf. Sanders 2000). In addition, it is probable that the "pulverizing" of bioclasts during high-energy events is associated with dissolution of very fine-grained calcium carbonate produced by abrasion. During deposition of the oolitic and oobioclastic limestones, minor amounts of abrasion and dissolution may have been active, but the very presence of well-preserved oolites indicates that precipitation and preservation of calcium carbonate prevailed in the oolite shoal belt. By comparison to recent active oolite bars, the scarcity of indigenous fossils is related to the hostility of shifting, medium to coarse sand to most epi- and endobenthic organisms, i.e., is original rather than a taphonomic result. Considering taphonomic loss and the original mineralogy of precipitates, the biocoenosis in the investigated section can be summarized as shown in Table 2.

Table 2 Biocoenosis as recorded by bioclasts and by biomurae, according to primary mineralogy (or inferred primary mineralogy) of shell or test

Aragonite
Phylloid algae
Bivalves
Gastropods
Dasycladalean algae
Magnesian calcite
Sessile epibiontic miliolines (e.g., *Ellesmerella*)
Vagile miliolines
Crinoids
Tubiphytes (magnesian calcite?)
Low-magnesian calcite
Benthic foraminifera (Fusulinina)
Microbialitic crusts of oncoids
Brachiopods (mainly productids)
Bryozoans (mainly fenestrates)
Recorded by biomuration
Bivalves and aragonitic algae (**platy fragments**)
Fleshy algae (**tubes**)
Small ?sponges

Bold typing indicates prevalent groups within each class

Benthic assemblages

Taking taphonomic loss into account, a semi-quantitative estimate of the life assemblages and taphonomic regimes in different habitats has been made (Fig. 7; Table 3). In a comparative analysis, Bush and Bambach (2004) estimated that, in Palaeozoic shelf assemblages, loss of original total diversity (alpha diversity) by syndepositional dissolution of aragonitic fossils averaged about 29%. This does not preclude that the abundance of aragonitic fossils may be lowered more than is obvious from total diversity (cf. Cherns and Wright 2000; Wright et al. 2003), as has also been documented from shell beds of the same depositional environment (Sanders 1999, 2001). For strictly quantitative reconstructions of taphonomic loss, the original relative percentage of aragonite relative to calcite had to be known (Sanders 2003; Bush and Bambach 2004). In Table 3, showing our reconstruction of benthic assemblages, we arranged each assemblage according to estimated original relative abundance of its elements. The estimate was based on observed abundance in thin sections, taking into account preferred loss of aragonitic fossils over calcitic fossils and vanished community elements recorded by

Table 3 Semi-quantitative reconstructions of shelf assemblages related to habitat and energy exposure

A Fleshy algal meadows
Fleshy algae (not preserved)
Epibiontic sessile foraminifera (mainly *Ellesmerella*)
Smaller benthic foraminifera
Bivalves
Brachiopods ≫
≪ Microgastropods
Phylloid algae
Dasycladalean algae
Bryozoans
Fusulinaceans
B Lime-muddy bioclastic sand
(substrate biotic coverage and relative percentage of community elements originally probably highly variable)
Fusulinaceans
Smaller benthic foraminifera
Bivalves
Gastropods, microgastropods
Brachiopods
Phylloid algae
Dasycladalean algae
Bryozoans
?Few crinoids
?Few *Tubiphytes*
C Oncoid "grounds"
(substrate biotic coverage and relative percentage of community elements originally probably highly variable)
Oncoids
Fusulinaceans
Sessile foraminifera
Smaller benthic foraminifera
Gastropods, microgastropods
Phylloid algae
Bryozoans
Tubiphytes
Richthofenids
D Phylloid algal meadows
Phylloid algae
Sessile foraminifera (incl. *Ellesmerella*)
Epibiontic bryozoans
Epibiontic microbialite crusts
Bivalves ≫
Microgastropods, gastropods ≫
Dasycladaleans
Brachiopods
Benthic bryozoans
E Ooid/ooid-bioclast sand bodies
No indigenous benthic assemblage indicated

Each reconstructed assemblage A to E is shown according to estimated relative abundance of community elements, from the top left column (most abundant elements) to lower right column (least abundant elements) (see also Fig. 6). Within each column, the vertical arrangement not necessarily reflects the relative abundance, particularly for assemblages B and C ≫ = potentially also less abundant; ≪ = potentially also more abundant

bioimmuration. Within each assemblage (Table 3), the certainty of the reconstructed relative abundance decreases with decreasing abundance.

By analogy to present low-energy gravelly shore zones, the beachface to uppermost shoreface probably was devoid of an indigenous benthic assemblage (Fig. 7; cf. Sanders 2000). For "lagoonal" to inner shelf environments, the different limestone facies record different communities (Table 3). In the ellesmerellites, the biomurae record community elements that had completely vanished, such as the inferred fleshy algae and small ?calcisponges, and elements that are underrepresented, such as bivalves. In recent carbonate environments, epibionts in seagrass meadows are a major source of biogenic calcium carbonate, including silt- to mud-sized sediment (e.g., Nelsen and Ginsburg 1986). Although seagrass-like plants exist only since the Early Cretaceous, we infer that the present case study represents a broadly similar situation: fleshy algal meadows that provided a substrate for calcium carbonate production by sessile epibiontic foraminifera. Based on the abundance of tube-shaped *Ellesmerella* fragments and taking into account that the standing stock of fleshy algae probably was not totally and always encrusted, we infer the existence of meadows of fleshy algae in low-energy, nearshore settings (Fig. 7, and A in Table 3). Because they were resistant to dissolution, brachiopods should be enriched in the *Ellesmerella* beds relative to the beds between; this is not the case, suggesting that brachiopods were a relatively subordinate part of that life assemblage. Due to marked taphonomic loss, bivalves are underrepresented. In addition, microgastropods may have suffered marked taphonomic loss, masking their potential presence as formerly more abundant elements of the benthic assemblage. For phylloid and dasycladalean algae, bryozoans, fusulinaceans and crinoids, we infer that their scarcity to absence reflects a genuine subordinance to absence in the benthic assemblage. For substrates of bioturbated, lime-muddy bioclast sand (= bioclastic wacke/packstones), and for lime-muddy bioturbated substrates rich in oncoids, similar to such substrate types in recent carbonate environments, we infer a variable, patchy distribution of prevalent benthos (Fig. 7, and B and C in Table 3). For substrates with oncoids, sessile epibenthos such as bryozoans, *Tubiphytes* and richthofenids are characteristic.

For deposits of former lime-muddy substrates colonized by phylloid algal meadows, giving rise to algal plate floatstones to bafflestones, the remains of epibenthic organisms (sessile foraminifera, bryozoans, *Ellesmerella*) are fairly common (D in Table 3). Because this epibenthos in many cases is attached to algal plates, it can be inferred that at least a large portion of the epibenthos thrived on phylloid algae; another portion, however, may have thrived on vanished substrates such as fleshy algae. Because in these limestones, evidence for taphonomic loss by abrasion and dissolution is absent, the comparatively few bivalves, (micro)gastropods and other sessile benthos probably represent a real former scarcity of these organisms. Where algal plates are not preserved *in situ*, taphonomic loss

by dissolution was high (see above). Finally, the habitats of ooid shoals and shifting oobioclastic sand close to or within fair-weather wave base, producing oolites and rounded bioclastic grainstones, were hostile to benthos.

Discussion

Substantial dissolution of calcium carbonate in the sediment of tropical, shallow subtidal settings is documented both for modern and ancient carbonate environments (Walter and Burton 1990; Ku et al. 1999; Sanders 2001; Powell et al. 2002). Dissolution is driven by bioturbation in interaction with organic matter oxidation and sulfate reduction (Walter et al. 1993; Ku et al. 1999). For the investigated section, aside of abrasion along the gravelly beach as a major agent of taphonomic loss, the degree of carbonate preservation and taphobias correlated with depositional setting (Fig. 7); this underscores that syndepositional dissolution is, in part at least, a function of substrate type and setting (Ku et al. 1999; Sanders 2003). Because of the low permeability of muddy substrates, chemical gradients necessary for dissolution can be maintained over a prolonged interval of time. In winnowed sands, by contrast, chemical gradients tend to be quickly eliminated by pore water flushing. Thus, during very early diagenesis, lime-muddy substrates are preferred loci of taphonomic loss by dissolution, while flushed sandy or reefal substrates are loci of prevalent precipitation and carbonate preservation (Fig. 7; Sanders 2003). Because the preserved sediment represents that what remained, however, packstone to grainstone texture *per se* do not rule out dissolution loss (Sanders 2004).

In four cases, for phylloid algal plates, quantitative reconstruction of the amount of algae dissolved yielded amounts ranging from zero, or nearly so, (Figs. 6C and D) up to about 65% (see captions to Figs. 10E–H) to nearly 100% removal. Taking a value of 65% removal (Fig. 10H), and a value of about 27% phylloid algal plates (Fig. 6C), this calculated to $27 \times 0.65 = 17.55\%$ lost. Even in case of wholesale removal (=27% in present example) of phylloid algal plates, the effect on final lithified thickness of the bed should be minor, and will be difficult to separate unequivocally from reduction of stratigraphic thickness by other processes, such as pressure solution (Sanders 2004). This "direct" approach can only take into account those bioclasts that still had left a readable record, whereas fossils that underwent complete destruction escape recognition. Moreover, the total amount of loss of calcium carbonate will be underestimated, since it is probable that a large yet unquantified amount of lime mud was dissolved, too. Finally, it is not known how much of the dissolved calcium carbonate reprecipitated within the sediment, as a fine-grained cement or epitaxial overgrowth, and how much was actually recycled to the sea (cf. Broecker and Clark 2003; Morse et al. 2003; Sanders 2003).

During the Palaeozoic, calcified forms of interpreted cyanobacterial origin, such as *Girvanella*, were important contributors to the sediment budget (Coniglio and James 1985; Pratt 2001). Pratt (2001) estimated that a single "calcification event" (perhaps one or several events per year; see Pratt 2001: 765) of a typical *Girvanella* biofilm yielded about 170 g/m^2 calcium carbonate, a value identical to that estimated by Robbins et al. (1997) to be potentially contributed, per annum and per square metre, by whitings to the sediment budget of the Bahama Banks (but see Morse et al. 2003). Encrusting foraminifera, many of them with tests of low-magnesian calcite, are known since the Ordovician (Taylor and Wilson 2003). In the Garnitzenbach section, the abundance of oncoids and of sessile foraminiferal crusts probably is related to an elevated nutrient level from terrestrial runoff, and/or to elevated alkalinity of the sea water near land. Cyanobacteria precipitate low-magnesian calcite (Riding 1991). In the ellesmerellites composed of curved platy fragments, a rough minimum estimate of the potential contribution of calcium carbonate can be made, by means of the method described above. For the image shown in Fig. 8B, the *larger* fragments constitute 16 vol% of the sediment; if a porosity of about 20% (constructional voids in the crusts) is subtracted, this amounts to at least 12.8 vol% contribution of calcium carbonate to the sediment. For ellesmerellites composed of platy fragments, a percentage at or close to the percentage of grain support (40-50%; Flügel 2004) must be assumed. Again, if subtracting an "intraskeletal" porosity of 20%, this indicates that about 32–40 vol% of platy ellesmerellites consist of foraminiferal calcite (the rest being cement and/or lime-muddy matrix). Taking into account that many *Ellesmerella* crusts are equally thick or thicker than their substrate, it is reasonable to suggest that the precipitation of epibiontic calcite compensated or even exceeded the loss of calcium carbonate imparted by dissolution of the aragonitic hardparts.

In addition, similar to calcified epibionts on extant seagrass (cf. Nelsen and Ginsburg 1986), the encrusting foraminifera on fleshy algae represented only a gain to the carbonate budget, since the fleshy algae were not part of this budget. Thus, at least for assemblages of type A, C and D (Table 3), calcium carbonate lost by dissolution of aragonitic hardparts was compensated in part, or perhaps exceeded, by gain of calcium carbonate of epibionts. In the described succession, taking into account all the potential processes that influenced the carbonate budget (Table 4), and the uncertainties in their quantification, it is only obvious that the net carbonate budget was positive, reflected in limestone deposition. The described sedimentary facies clearly indicate that epibiontic calcium carbonate took a significant share in upholding a positive budget (cf. Fig. 7).

The present paper implies that non-calcified encrustation substrates, probably mainly plants, may have represented an important element of shallow-marine communities at least since the Late Palaeozoic, by providing a habitat to benthic communities and a substrate for calcifying epibionts. Epibiontic calcium carbonate mostly is low-magnesian calcite (foraminifera, bryozoans, cyanobacteria). Calcified epibionts thus represent a significant and, in some habitats, prevalent source of mineralogically stable low-magnesian calcite. Epibiontic calcification probably

Table 4 Processes that influenced the shallow neritic carbonate budget, upper Grenzland Formation to lower Zweikofel Formation

(1) $CaCO_3$ gain
Precipitation
Ooid formation
Biogenic precipitation (microbialites, shells, tests, skeletons)
Reprecipitation of early-dissolved $CaCO_3$ within the sediment
?Whitings/?epitaxial carbonate precipitation
To-site transport
Alongshelf transport of carbonate sediment (hypothetical)
(2) $CaCO_3$ loss
Dissolution
Dissolution in sea water (along beachface)
Dissolution in bioturbated, soft to firm, lime-muddy substrata
Bioerosion
Microboring (common)
Macroboring (very scarce)
Off-site transport
Alongshelf transport (hypothetical) and offshelf transport of carbonate sediment

See text for discussion

compensated, in part at least or perhaps more than enough, for loss of calcium carbonate imparted by syndepositional dissolution. The contemporaneous action, to a different amount in different habitats, of both carbonate dissolution and precipitation yet impedes a straightforward approach towards establishing ancient carbonate sediment budgets.

Conclusions

1. During the Early Permian, in the Carnic Alps, emergent areas were fringed by quartz-gravelly beaches. Seaward, a low-energy lime-muddy "lagoon" was present that was inhabited by fleshy algae, calcareous algae, molluscs and benthic foraminifera. Farther offshore, a belt of ooid shoals was situated ahead of a slightly deeper subtidal, low-energy carbonate inner shelf.
2. Five main habitats are distinguished. (1) Low-energy lagoonal meadows of fleshy algae that were encrusted by *Ellesmerella* and other sessile foraminifera. (2) Lagoon and inner shelf, lime-muddy bioclastic sand (wkst, pkst) populated by foraminifera, molluscs, brachiopods, and calcareous green algae. (3) Lagoon and inner shelf, lime-muddy bioclastic sand with oncoids. The oncoid areas were habitat mainly to fleshy algae, sessile and vagile foraminifera, molluscs and calcareous algae. (4) Phylloid algal meadows with the algae locally overgrown by sessile foraminifera (e.g., *Ellesmerella*) and bryozoans. (5) Shoals of ooids or of ooid-bioclast sand.
3. Along the gravelly beach, abrasion of bioclasts as well as winnowing and (partial) dissolution of fine-grained bioclastic calcium carbonate resulted in near-complete taphonomic loss. In lagoonal and inner shelfal, lime-muddy to lime-muddy/argillaceous substrates, dissolution of aragonitic bioclasts led to variable, moderate to strong tapholoss. For ooid shoals, no tapholoss by dissolution is recorded.
4. For the desribed Permian lagoonal and shallow shelfal habitats, tapholoss is recorded mainly by sessile foraminiferal crusts. The foraminifera had encrusted substrates that subsequently vanished, either, by rotting (fleshy algae), or by dissolution of aragonitic bioclasts.
5. While many aragonitic bioclasts were partly or completely dissolved, the magnesian calcitic and calcitic tests of epibionts escaped dissolution. The epibiontic source of calcium carbonate was significant, and perhaps compensated to, locally, exceeded the loss imparted by dissolution.

Acknowledgements Paul Wright, Cardiff, and Oliver Weidlich, London, are thanked for constructive reviews.

References

Algeo TS, Wilkinson BH (1988) Periodicity of mesoscale Phanerozoic sedimentary cycles and the role of Milankovitch orbital modulation. J Geol 96:313–322

Baars DL, Torres AM (1991) Late Paleozoic phylloid algae - a pragmatic review. Palaios 6:513–515

Broecker WS, Clark E (2003) Pseudo dissolution of marine calcite. Earth Planet Sci Lett 208:291–296

Buggisch W, Flügel E, Leitz F, Tietz G-F (1976) Die fazielle und paläogeographische Entwicklung im Perm der Karnischen Alpen und in den Randgebieten. Geol Rundsch 65:649–690

Burchette TP, Riding R (1977) Attached vermiform gastropods in Carboniferous marginal marine stromatolites and biostromes. Lethaia 10:17–28

Bush AM, Bambach RK (2004) Did alpha diversity increase during the Phanerozoic? Lifting the veils of taphonomic, latitudinal, and environmental biases. J Geol 112:625–642

Cherns L, Wright VP (2000) Missing molluscs as evidence of large-scale early skeletal aragonite dissolution in a Silurian sea. Geology 28:791–794

Coniglio M, James NP (1985) Calcified algae as sediment contributors to Early Paleozoic limestones: evidence from deep-water sediments of the Cow Head Group, western Newfoundland. J Sediment Petrol 55:746–754

Flügel E (1971) Palökologische Interpretation des Zottachkopf-Profiles mit Hilfe von Kleinforaminiferen (Oberer Pseudoschwagerinen-Kalk, unteres Perm: Karnische Alpen). Carinthia II, Sonderh 28:61–96

Flügel E (1974) Fazies-Interpretation der unterpermischen Sedimente in den Karnischen Alpen. Carinthia II, 164(84):43–62

Flügel E (1977) Environmental models for Upper Paleozoic benthic calcareous algal communities. In: Flügel E (ed) Fossil algae. Springer, Berlin, pp 314–343

Flügel E (2004) Microfacies of carbonate rocks. Springer, Berlin

Flügel E, Flügel-Kahler E (1980) Algen aus den Kalken der Trogkofel-Schichten der Karnischen Alpen. In: Flügel E (ed) Die Trogkofel-Stufe im Unterperm der Karnischen Alpen. Carinthia, Sonderh 36:113–182

Flügel E, Homann W, Tietz G-F (1971) Litho- und Biofazies eines Detailprofils in den Pberen Pseudoschwagerinen-Schichten (Unter-Perm) der Karnischen Alpen. Verh Geol Bundesanst 1971:10–42

Flügel E, Fohrer B, Forke H, Krainer K, Samankassou E (1997) Cyclic sediments and algal mounds in the Upper Paleozoic of the Carnic Alps. Gaea Heidelberg 4:79–100

Forke HC (1995) Biostratigraphie (Fusulinaceanen; Conodonten) und Mikrofazies im Unterperm (Sakmar) der Karnischen Alpen (Naßfeldgebiet, Österreich). Jb Geol Bundesanst 138:207–297

Frakes LA, Francis JE, Syktus JI (1992) Climate modes of the phanerozoic. Cambridge University Press, Cambridge

Hampson GJ (2000) Discontinuity surfaces, clinoforms, and facies architecture in a wave-dominated, shoreface-shelf parasequence. J Sediment Res 70:325–340

Homann W (1972) Unter- und tief-mittelpermische Kalkalgen aus den Rattendorfer Schichten, dem Trogkofel-Kalk und dem Treßdorfer Kalk der Karnischen Alpen (Österreich). Senckenberg Lethaea 53:135–313

Kochansky-Devidé V (1973) *Ramovsia limes* n. gen. n. sp. (Problematica), ein Leitfossil der Grenzlandbänke (unteres Perm). N Jb Geol Paläont Mh 1973/8:462–468

Krainer K (1992) Fazies, Sedimentationsprozesse und Paläogeographie im Karbon der Ost- und Südalpen. Jb Geol Bundesanst 135:99–193

Krainer K, Davydov V (1998) Facies and biostratigraphy of the Late Carboniferous/Early Permian sedimentary sequence in the Carnic Alps (Austria/Italy). Geodiversitas 20:643–662

Ku TCW, Walter LM, Coleman ML, Blake RE, Martini AM (1999) Coupling between sulfur recycling and syndepositional carbonate dissolution: Evidence from oxygen and sulfur isotope composition of pore water sulfate, South Florida Platform, U.S.A. Geochim Cosmochim Acta 63:2529–2546

Manzoni M, Venturini C, Vigliotti L (1989) Paleomagnetism of Upper Carboniferous limestones from the Carnic Alps. Tectonophysics 165:73–80

Morse JW, Gledhill DK, Millero FJ (2003) $CaCO_3$ precipitation kinetics in waters from the Great Bahama Bank: Implications for the relationship between Bank hydrochemistry and whitings. Geochim Cosmocim Acta 67:2819–2826

Moulin E, Jordens A, Wollast R (1985) Influence of the aerobic bacterial respiration on the early dissolution of carbonates in coastal sediments. Proc Progr Belgian Oceanogr Res, March 1985, pp 196–208

Murray JW, Alve E (1999) Natural dissolution of modern shallow water benthic foraminifera: taphonomic effects on the palaeoecological record. Palaeogeogr Palaeoclimatol Palaeoecol 146:195–209

Nelsen JE Jr, Ginsburg RN (1986) Calcium carbonate production by epibionts on *Thalassia* in Florida Bay. J Sediment Petrol 56:622–628

Palmer TJ, Hudson JD, Wilson MA (1988) Palaeoecological evidence for early aragonite dissolution in ancient calcite seas. Nature 335:809–810

Pattison SAJ (1995) Sequence stratigraphic significance of sharp-based lowstand shoreface deposits, Kenilworth Member, Book Cliffs, Utah. Amer Assoc Petrol Geol Bull 79:444–462

Plint AG (1988) Sharp-based shoreface sequences and "offshore bars" in the Cardium Formation of Alberta: their relationship to relative changes in sea level. In: Wilgus CK, Hastings BS, Ross CA, Posamentier H, Kendall CGStC (eds) Sea-level changes - an integrated approach. SEPM Spec Publ 42:357–370

Powell EN, Parsons-Hubbard KM, Callender WR, Staff GM, Rowe GT, Brett CE, Walker SE, Raymond A, Carlson DD, White S, Heise EA (2002) Taphonomy on the continental shelf and slope: two-year trends - Gulf of Mexico and Bahamas. Palaeogeogr Palaeoclimatol Palaeoecol 184:1–35

Pratt BR (2001) Calcification of cyanobacterial filaments: *Girvanella* and the origin of lower Paleozoic lime mud. Geology 29:763–766

Riding R (1991) Calcified cyanobacteria. In: Riding R (ed) Calcareous algae and stromatolites. Springer, Berlin, pp 55–87

Robbins LL, Tao Y, Evans CA (1997) Temporal and spatial distribution of whitings on Great Bahama Bank and a new lime mud budget. Geology 25:947–950

Rodriguez S (2004) Taphonomic alterations in upper Viséan dissepimented rugose corals from the Sierra del Castillo unit (Carboniferous, Córdoba, Spain). Palaeogeogr Palaeoclimatol Palaeoecol 241:135–153

Ross CA, Ross JRP (1985) Late Paleozoic sequences are synchronous and worldwide. Geology 13:194–197

Samankassou E (2002) Cool-water carbonates in a paleoequatorial shallow-water environment: The paradox of the Auernig cyclic sediments (Upper Pennsylvanian, Carnic Alps, Austria-Italy) and its implications. Geology 30:655–658

Sanders D (1999) Shell disintegration and taphonomic loss in rudist biostromes. Lethaia 32:101–112

Sanders D (2000) Rocky shore-gravelly beach transition, and storm/post-storm changes of a Holocene gravelly beach (Kos island, Aegean Sea): Stratigraphic significance. Facies 42:227–244

Sanders D (2001) Burrow-mediated carbonate dissolution in rudist biostromes (Aurisina, Italy): implications for taphonomy in tropical, shallow subtidal carbonate environments. Palaeogeogr Palaeoclimatol Palaeoecol 168:41–76

Sanders D (2003) Syndepositional dissolution of calcium carbonate in neritic carbonate environments: Geological recognition, processes, potential significance. J African Earth Sci 36:99–134

Sanders D (2004) Potential significance of syndepositional carbonate dissolution for platform banktop aggradation and sediment texture: a graphic modeling approach. Austrian J Earth Sci 95/96:71–79

Scotese CR, Boucot AJ, McKerrow WS (1999) Gondwanan palaeogeography and palaeoclimatology. J African Earth Sci 28:99–114

Stanley SM, Hardie LA (1998) Secular oscillations in the carbonate mineralogy of reef-building and sediment-producing organisms driven by tectonically forced shifts in seawater chemistry. Palaeogeogr Palaeoclimatol Palaeoecol 144:3–19

Taylor PD, Wilson MA (2003) Palaeoecology and evolution of marine hard substrate communities. Earth Sci Rev 62:1–103

Vachard D, Krainer K (2001) Smaller foraminifers, characteristic algae and pseudo-algae of the latest Carboniferous - Early Permian Rattendorf Group, Carnic Alps (Austria/Italy). Riv Ital Paleont Stratigr 107:169–195

Venturini C (1982) Il bacino tardoercinico di Pramollo (Alpi Carniche): Un evoluzione regolata della tettonica sinsedimentaria. Mem Soc Geol Ital 24:23–42

Venturini C (1991) Introduction to the geology of the Pramollo basin (Carnic Alps) and its surroundings. Giorn Geol 3A, 53:13–47

Voigt E (1966) Die Erhaltung vergänglicher Organismen durch Abformung infolge Inkrustation durch sessile Tiere. N Jb Geol Paläont Abh 125:401–422

Walter LM, Burton EA (1990) Dissolution of Recent platform carbonate sediments in marine pore fluids. Amer J Sci 290:601–643

Walter LM, Bischof SA, Patterson WP, Lyons TL (1993) Dissolution and crystallization in modern shelf carbonates: Evidence from pore water and solid phase chemistry. Phil Trans R Soc London A 344:27–36

Weedon MJ (1990) Shell structure and affinity of vermiform gastropods. Lethaia 23:297–309

Weedon MJ (1991) Microstructure and affinity of the enigmatic Devonian tubular fossil *Trypanipora*. Lethaia 24:227–234

Wright P, Cherns L, Hogdes P (2003) Missing molluscs: field testing taphonomic loss in the Mesozoic through early large-scale aragonite dissolution. Geology 31:211–214